JTTEE5 17:655–661
DOI: 10.1007/s11666-008-9264-3
1059-9630/$19.00 © ASM International

Introduction to High-Velocity Suspension Flame Spraying (HVSFS)

Rainer Gadow, Andreas Killinger, and Johannes Rauch

(Submitted May 14, 2008; in revised form October 2, 2008)

High-velocity suspension flame spraying (HVSFS) has been developed to thermally spray suspensions containing micron, submicron, and nanoparticles with hypersonic speed. For this purpose, the suspension is introduced directly into the combustion chamber of a modified HVOF torch. The aim in mind is to achieve dense coatings with a refined microstructure. Especially from nanostructured coatings superior physical properties are expected for many potential applications. Direct spraying of suspensions offers flexibility in combining and processing different materials. It is a cost-saving process and allows the allocation of entirely new application fields. The paper gives an overview of the HVSFS spray method and will present some actual results that have been achieved by spraying the nanooxide ceramic materials Al_2O_3, TiO_2, 3YSZ, and Cr_2O_3.

Keywords nanocrystalline composites, nanopowders, nanostructured materials

1. Introduction

Thermal spray technology has been applied for decades with great success and still bears a great potential for new applications in many industrial fields. One of the great benefits is the wide variety of spray materials that can be applied to all kind of substrate materials.

However, standard spray techniques face restrictions regarding their coating thickness and resulting microstructure. From the fact that the processed spray material (rods, wires, or standard spray powders) results in spray particles with a certain particle size that cannot be reduced, there are limitations to decreasing coating thickness significantly below a value in the range of 30 μm because individual splats are too coarse to form a homogeneous and sealed coating structure. For most applications, a coating thickness of 200 to 300 μm matches well with the technical requirements; however, there are new applications where thin coatings in the range of 5 to 50 μm would be of great interest, for example, in the field of sensor technology, in the development of solid electrolytes (e.g., for solid oxide fuel cell, or SOFC), and for a new generation of nanostructured tribocoatings.

A reduction of particle sizes below 5 μm means an extraordinary effort in powder feeding technique, as fluidization of the spray powder gets more and more challenging with a decreasing particle size. Therefore, suspensions seem to offer a promising solution of this problem. Moreover, using a suspension opens up a completely new field of specially designed spray materials, including nanopowders that are currently not available on the spray powder market. The processing of a nanopowder using the standard thermal spray procedure first of all requires the agglomeration of the nanopowders by a spray drying process to form spray particles with appropriate grain size that are suitable for a standard powder feeding device. These powder qualities are expensive and not available on the market for every combination of materials. Oxide-based materials are supplied by several companies, whereas cermet-based powder materials containing nanosized hard-phase particles such as carbides or borides are relatively rare and expensive. Spraying these powder types, however, leads to spray particles with particle diameters comparable to standard spray powders. The aim to form thin-film spray coatings with a refined internal coating structure cannot be solved by this approach, although (in the case of mixed-phase powders) a dispersion of submicron or even nanoscaled hard phases can be realized. A general problem is the fact that during the melting process in the flame, the agglomerated particles lose their nanostructure (in the case of a single-phase agglomerate), so it is not yet clear if there is any benefit compared to using standard powders.

Suspension spraying has been carried out using plasma spraying, flame spraying, and high-velocity oxyfuel (HVOF) (Ref 1-4). In the case of plasma spraying, the injection of the liquid generally is performed perpendicular

This article is an invited paper selected from presentations at the 2008 International Thermal Spray Conference and has been expanded from the original presentation. It is simultaneously published in *Thermal Spray Crossing Borders, Proceedings of the 2008 International Thermal Spray Conference*, Maastricht, The Netherlands, June 2-4, 2008, Basil R. Marple, Margaret M. Hyland, Yuk-Chiu Lau, Chang-Jiu Li, Rogerio S. Lima, and Ghislain Montavon, Ed., ASM International, Materials Park, OH, 2008.

Rainer Gadow, Andreas Killinger, and **Johannes Rauch**, Institute for Manufacturing Technologies of Ceramic Components and Composites (IFKB), University of Stuttgart, Allmandring 7b, D-70569 Stuttgart, Germany. Contact e-mail: rainer.gadow@ifkb.uni-stuttgart.de.

to the plasma flame. In the case of conventional flame and HVOF spraying, an axial injection into the flame or combustion chamber respectively is preferred as it circumvents the problem of strong flame disturbance causing instabilities in the spray process (Ref 1).

Introducing a liquid into the spray process raises some basic problems. Any liquid, being water or an organic solvent, starts to evaporate rapidly when introduced into the flame causing two important effects: (i) a significant cooling of the flame and (ii) a strong disturbance of the free expanding hot gas stream caused by the expanding vapor through the evaporation process, as is especially the case in plasma spraying. When the vapor is introduced into a combustion chamber, a significant rise of the combustion chamber pressure will occur as can be observed in the high-velocity suspension flame spraying (HVSFS) process.

Particle size strongly influences the particle thermal history. Small particles rapidly heat up, but they also rapidly cool down, resulting in a far different behavior concerning the splat formation on the surface. It also affects interlamellar adhesion of the splats and thereby influences the mechanical properties (e.g., Young's modulus, hardness) of the coating. When thermal spraying suspensions, the liquid is fragmented through an atomization process into small droplets not necessarily having the size of the primary particles (e.g., nanoparticles); this issue has been extensively discussed in literature (Ref 5). It has been reported for plasma spraying of suspensions (Ref 6), but can also be observed in the HVSFS process, as shown by the authors in Ref 4. The goal is to optimize the atomization in the combustion chamber to achieve the smallest suspension droplets possible. This leads to finer splats in the coating with the above-described improvements.

2. Experimental

The principle of HVSF spraying has been introduced and described in our recent publication (Ref 4); an improved configuration of the HVSFS equipment is shown in Fig. 1. It consists of a suspension container connected to a pump feeder system. A flexible suspension line feeds the suspension axially and concentrically into the combustion chamber of a modified HVOF gun. A second container holds the pure solvent to flush the suspension line and injection nozzle when shutting down the process. The HVSFS torch is based on a TopGun-G system (manufactured by GTV, GTV Verschleiss-Schutz GmbH Gewerbegebiet "Vor der Neuwiese", Luckenbach) and has been modified to meet suspension spray requirements. Major modifications concern a suspension injection nozzle that is capable of evenly injecting a suspension into the combustion chamber of the HVSFS torch. The injection nozzles have a smaller diameter than those used in conventional HVOF torches. Two different shapes, cylindrical and conical, were used. It was found that cylindrical injection nozzle geometries show a strong tendency to clog during the process, whereas a conical geometry allows a stable coating process.

Propane and ethene were preferentially chosen as combustion fuels as they allow stable operation of the HVSFS process. Basically, using acetylene can be of advantage when spraying oxide materials, as it delivers higher flame temperatures (Ref 7). However, with the insertion of liquid fuel, the combustion chamber pressure rises significantly, exceeding the maximum gas line pressure of 1.5 bar that is allowed for acetylene; therefore, expensive high-pressure lines would be necessary to run a stable HVSFS process.

For all suspensions, isopropanol was chosen as the organic solvent. Although stabilization of particles is more difficult than in aqueous media, this alcohol delivers fairly high enthalpy values during the combustion process. In case of the TiO_2, the suspension also contained water (10 wt.% of liquid phase) to optimize the viscosity by using the dispersing agent Dolapix CE64 (Zschimmer und Schwarz GmbH & Co KG, Chemische Fabriken, Lahnstein/Rhein).

3. Preparation of the Suspensions

Table 1 summarizes all powders used in this work. In a first step, the powders were attrition milled in isopropanol

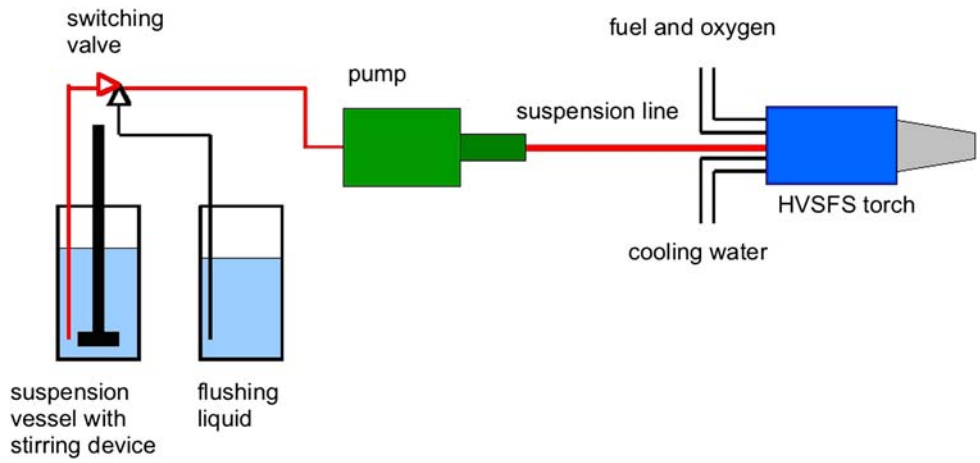

Fig. 1 Experimental setup for HVSFS (pump-based system)

solvent to force deagglomeration and particle breakup. This is necessary because most nanopowders show agglomerates with grain sizes that might clog the suspension injection nozzle (diameter 0.3-0.5 mm). To remove milling balls and possible agglomerates, the suspensions were sieved after milling process with a mesh of 50 µm. Suspensions were then applicable for spraying. The solid content of all suspensions in this work was in the range of 15 to 20 wt.%. A summary of the suspension compositions is given in Table 2.

Table 1 Summary of applied powder materials

Brand name (manufacturer)	Chemical composition	Primary grain size, nm	Phases analysis derived from XRD
TM-DAR (Taimei Chemicals)	n-Al_2O_3	150	α-Al_2O_3
Aeroxide P25 (Degussa)	n-TiO_2	15	Anatase, rutile
Nanofiller (DGTec)	n-Cr_2O_3	100	Eskolaite
VP PH (Degussa)	n-3YSZ	15	Tetragonal, monoclinic

Table 2 Composition of the different suspensions

Suspension	Solid content, wt.%	Isopropanol content, wt.%	Additives
n-Al_2O_3	20	80	HNO_3
n-TiO_2	10	90/10	Dolapix CE64
n-Cr_2O_3	15	85	HNO_3
n-3YSZ	20	80	HNO_3

Table 3 Parameters for HVSFS

Suspension	Fuel gas, slpm	O_2, slpm	Torch speed, mm/s	No. of cycles	Spray distance, mm	Feeding rate, g/min
n-Al_2O_3	P 65	350	600	10	150	10
n-TiO_2	P 50	220	800	10	100	8
n-Cr_2O_3	P 65	350	600	5	125	8
n-Cr_2O_3	E 90	300	600	5	125	8
n-3YSZ	E 90	300	600	10	120	10

P, propane; E, ethene

4. Coating Experiments

All suspensions were sprayed using propane or ethene as fuel gases; relevant spray parameters are summarized in Table 3. When choosing propane as a fuel gas, it was found that an oxygen/fuel ratio adjusted to approximately 5.4 achieved the best deposition rates. In case of ethene, the oxygen/fuel ratio was approximately 3.3. It should be kept in mind that flame temperature is strongly influenced by the presence of isopropanol in the flame. It also strongly changes the oxidation behavior of the flame.

Coatings were applied either on planar mild steel (St37) or aluminum alloy (AlMg3) samples (50 × 50 mm) and were mounted vertically on a sample holder. The HVSFS torch was operated on a six-axis robot system using a simple meander kinematic with a 1 mm offset. Sample cooling was performed using two air nozzles mounted on the torch. Substrate preparation prior to spraying included degreasing of the surface with acetone. For all substrates, a mild injection grit-blasting operation was carried out using white corundum particles (FEPA 120; ø = 100 to 125 µm) and 5 bar compressed air. Spray parameters are given in Table 3.

5. Characterization of the HVSFS Sprayed Coatings

From all samples, cross sections were prepared for image analysis using light microscopy and/or scanning electron microscopy (SEM). Surface topography was taken in SEM to reveal the structure of single splats. Microhardness was measured on coating cross section using a Fisherscope equipped with a Vickers indenter. All measurements are performed dynamically (universal hardness) according to DIN 50359-1. The given values are the average of 10 indentations. Coating porosity was determined from digital image analysis (Software AQUINTO, Analysis Software, Olympus Deutschland GmbH, Hamburg). Surface roughness was measured using a contact profilometer (Perthometer Concept, Mahr, Mahr GmbH Esslingen, Esslingen), R_z and R_a values were determined according to DIN EN ISO 4287. All results are summarized in Table 4.

5.1 Al_2O_3

Aluminum oxide suspension was HVSF sprayed on aluminum substrate using propane as fuel gas. A conical-shaped injection nozzle was used. The feeding rate was

Table 4 Mechanical and structural data of the HVSF sprayed coatings

Spray material	Vickers hardness	Coating porosity, %	R_z, µm	R_a, µm	Phase composition derived from XRD
n-Al_2O_3	620-880 $HV_{0.1}$, SD = 76	5	3.14	0.58	Mainly γ
n-TiO_2	~1000 $HV_{0.05}$	0-0.5	3.5	0.65	Mainly anatase
n-Cr_2O_3 propane	1400-1800 $HV_{0.01}$, SD = 145	4-5	2.75	0.47	Hexagonal
n-Cr_2O_3 ethene	1100-2000 $HV_{0.01}$, SD = 283	7-10	2.79	0.48	Hexagonal
n-3YSZ	715-816 $HV_{0.03}$, SD = 38	<1	8.68	1.75	Tetragonal

SD, standard deviation

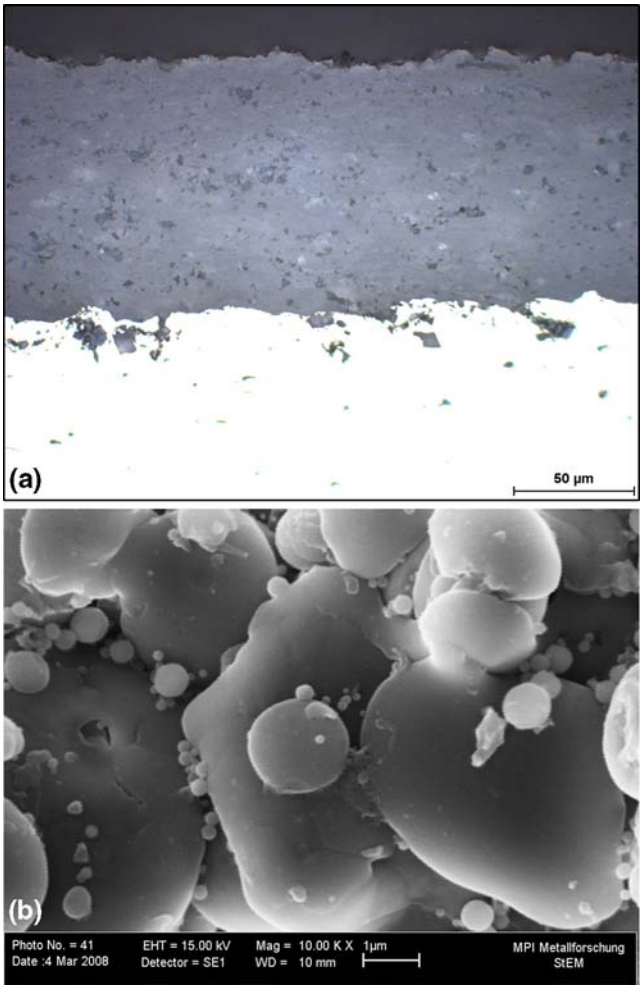

Fig. 2 (a) Light microscope image of HVSF sprayed Al_2O_3 coating. (b) SEM image of the coating surface

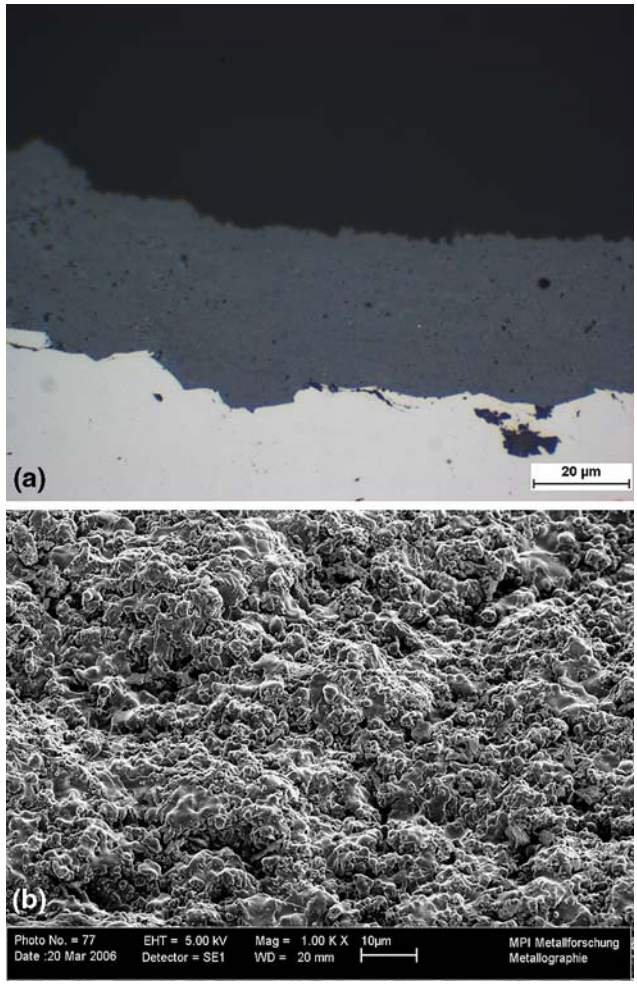

Fig. 3 (a) Light microscope image of HVSF sprayed TiO_2 coating. (b) SEM image of the coating surface

approximately 10 g/min, and the coating thickness was about 100 µm. Deposition rate was approximately 10 µm per transition. The alumina coating exhibits a good adhesion to the aluminum substrate (Fig. 2a). The porosity was approximately 5%; microhardness was in the range of 600 to 900 $HV_{0.1}$.

The coating surface shows fully molten droplets in the range of 1 to 5 µm, in the intersplat region small spherical particles with a size of 200 up to 500 nm are visible (Fig. 2b). Surface roughness is $R_z = 3.14$ µm and $R_a = 0.58$ µm.

5.2 TiO_2

The titanium oxide suspension was HVSF sprayed on aluminum substrate using propane as a fuel gas. The feeding rate was approximately 8 g/min; a conically shaped 0.3 mm nozzle was used. The applied coating thickness was approximately 30 µm; deposition rate was approximately 4 µm/cycle. In cross section, the TiO_2 coating appears with a very low porosity (Fig. 3a). The coating appears homogeneous; no internal structure is visible in cross section, and no unmolten particles are detected. The SEM surface image reveals fully molten splats ranging from a few 100 nm up to 10 µm with a good intersplat connection (Fig. 3b).

From the x-ray diffraction (XRD) data, it can be stated that the main fraction of the coating consists of anatase (approximately 75%); the rest of the material consists of rutile.

5.3 Cr_2O_3

Chromium oxide suspension was HVSF sprayed with propane and ethene to compare the influence of the fuel gases. Suspension feeding rate, torch setup, robot kinematics, and substrate were identically for both coatings, refer to Table 3. The n-Cr_2O_3 suspension was sprayed on steel substrates with a feeding rate of approximately 8 g/min using a cylindrically shaped 0.4 mm nozzle. Deposition rate was in the range of 2 µm/cycle for both fuel gases. The achieved coating has a thickness of 10 to 15 µm, exhibits good adhesion to the steel substrate, and shows a porosity of approximately 5% in the case of propane and approximately 10% in case of ethene; refer to Fig. 4(a) and 4(b); for porosity data see Table 4.

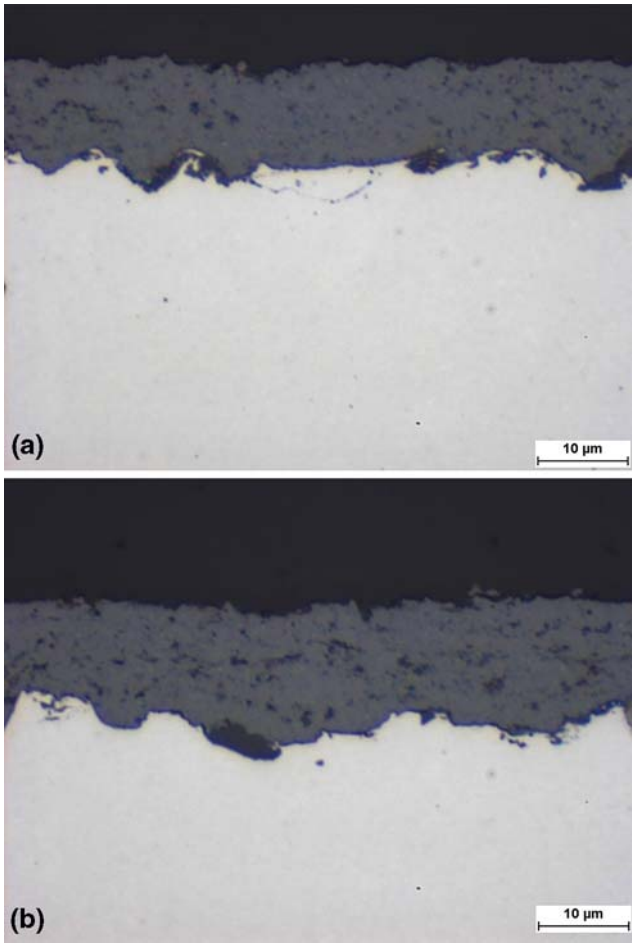

Fig. 4 Light microscope images of HVSF sprayed chromium oxide cross sections. (a) Sprayed with fuel gas: propane. (b) Sprayed with fuel gas: ethene

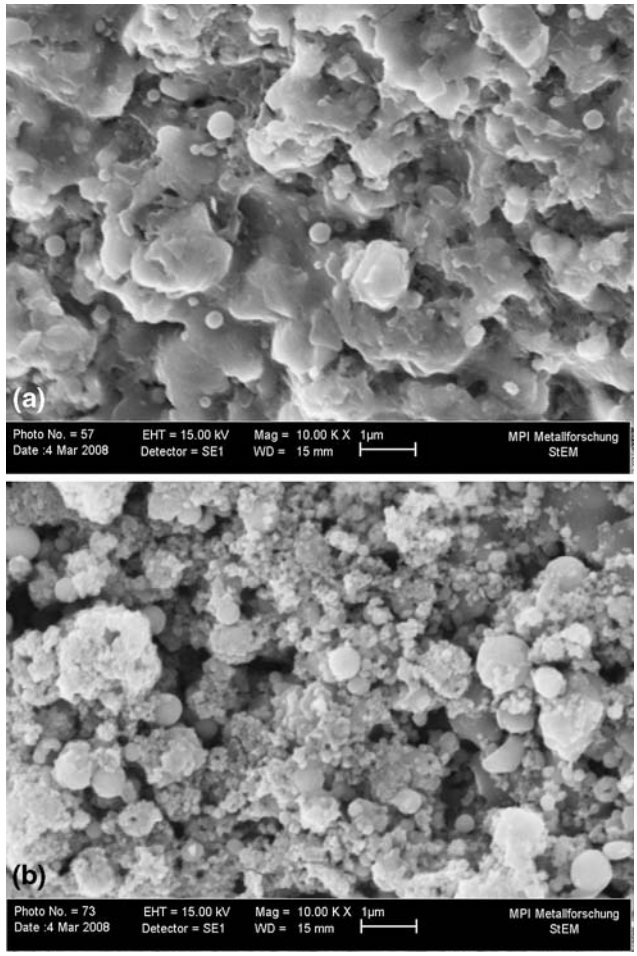

Fig. 5 SEM images of HVSF sprayed chromium oxide surfaces. (a) Fuel gas: propane. (b) Fuel gas: ethene

The microhardness of the propane sprayed coating was in the range 1400 to 1800 $HV_{0.01}$; hardness of the ethene sprayed coating was in the range of 1100 to 2000 $HV_{0.01}$. In case of the ethene sprayed samples, the lower microhardness corresponds to the higher porosity in the coating. There is a fairly high variance of the measured values due to the low indenter forces.

In SEM, coatings show different surface structures. The surface of the coating sprayed with propane appears coarser with fully molten droplets in the range of 1 to 3 µm (Fig. 5a). A refined splat structure is visible on the ethene sprayed coating surface (Fig. 5b). Small spherical droplets in the range of 100 nm are present together with larger droplets (1 to 3 µm). The surface roughness of both coatings is comparable; $R_z = 2.75$ µm, $R_a = 0.47$ µm for the propane sprayed, and $R_z = 2.79$ µm, $R_a = 0.48$ µm for the ethene sprayed.

5.4 3YSZ

The YSZ suspension was flame sprayed on steel substrate with a feeding rate of approximately 10 g/min using a 0.4 mm conical nozzle. In this case, ethene was chosen as the fuel gas to achieve a high flame temperature. The deposition rate was in the range of 3 µm/cycle. In cross sections, the YSZ coating appears dense and homogeneous. The thickness of the coating is about 30 µm (Fig. 6a). In SEM images stretched pores with a diameter of about 200 nm are visible (Fig. 6b). The microhardness of the coating was measured 766 $HV_{0.03}$. From XRD it can be stated that the coating consists of a pure tetragonal phase.

The surface of the 3YSZ coating appears as a fully molten splat structure with splats in the range of 1 to 3 µm and a well-established intersplat connection. Fine spherical particles with a diameter of 50 to 200 nm are distributed between the larger agglomerates (Fig. 7a and b). The surface roughness was measured to $R_z = 8.68$ µm and $R_a = 1.75$ µm.

6. Discussion

All HVSF sprayed coatings exhibit a refined splat structure that is at least one order of magnitude below standard spray coatings. This is also valid for the pore

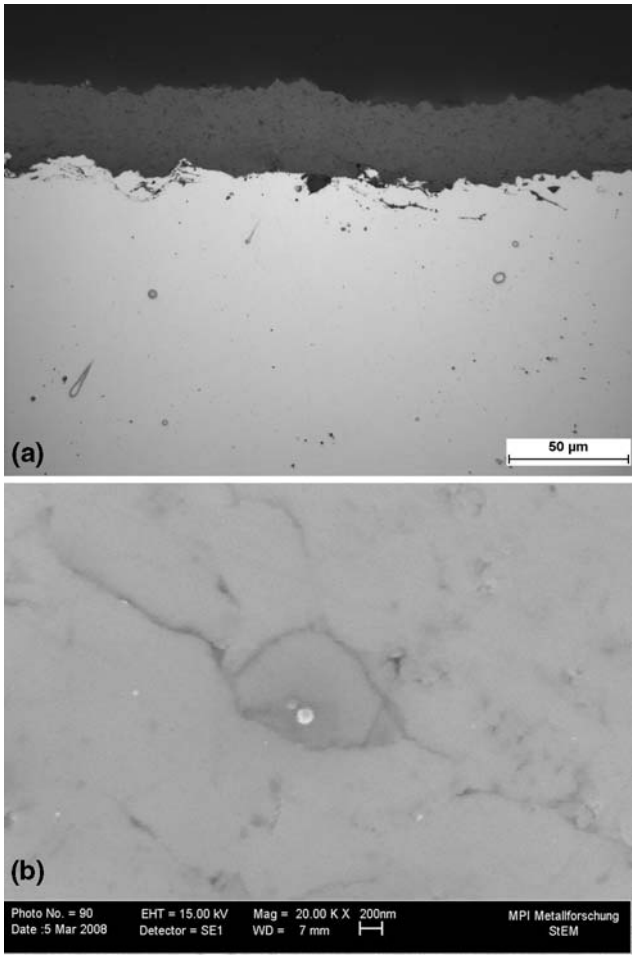

Fig. 6 (a) Light microscope image of a HVSF sprayed 3YSZ coating. (b) SEM image of HVSF sprayed 3YSZ, pore structures are in the range of 50 nm

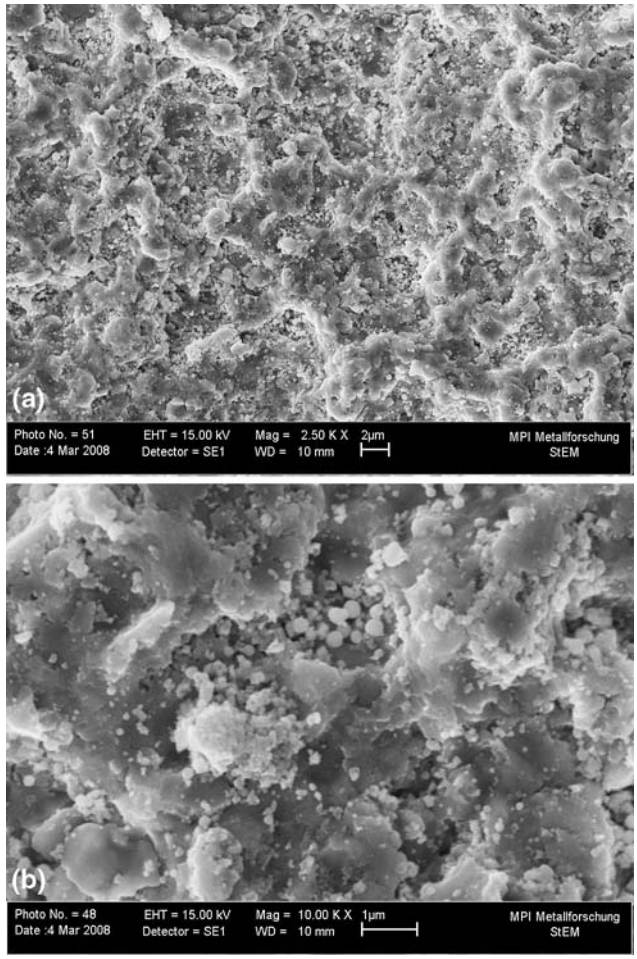

Fig. 7 SEM images of the surface of HVSF sprayed 3YSZ at different orders of magnitude

structure. Therefore, all HVSF sprayed coatings exhibit remarkably low values of surface roughness. From all investigated coatings, the titanium and zirconium oxide coatings exhibit lowest porosity values.

Generally, there is a fairly high variance of the measured hardness values because of the reduced coating thickness in chromium and zirconium oxide; further investigations will include nanoindenter analysis to achieve more precise values for coatings below 50 µm.

For all coatings, there is no visible evidence that particles were insufficiently molten. So far, there is no clear tendency that porosity would directly correspond to the melting point of the sprayed material, titanium oxide (melting point 1800 °C) and 3YSZ (melting point 2700 °C) show highest densities. Deposition efficiency is in the range of 3 to 4 µm/cycle for all investigated suspensions. So far, using ethene as a fuel gas providing a higher flame temperature did not show any advantage concerning the deposition efficiency and coating porosity achieved in the HVSFS process.

From XRD data, it is found that a crystallite structure in the coating significantly exceeds the size of the initial nanopowders. However, from our earlier publication it was found that spraying of mixed nanooxides can preserve a nanostructure in the coating (Ref 8).

7. Summary

The HVSFS method was evaluated to manufacture coatings from n-Al_2O_3 n-TiO_2, n-Cr_2O_3, n-3YSZ nanooxides. Appropriate suspensions were prepared in-house using isopropanol as a solvent. All materials were sprayed using propane or ethene as a fuel gas.

For all investigated materials, homogeneous oxide coatings featuring a significantly lower surface roughness and a highly refined microstructure compared to standard spray coatings could be manufactured. So far, measured microhardness values are comparable or slightly lower than those of standard coatings, but nanoindenter measurements are required to further characterize the coatings more precisely. All coatings clearly show a crystalline structure in XRD.

References

1. R. Gadow, A. Killinger, M. Kuhn, and D. Lopéz, Published patent application DE 10,2005,038,453 A1, 2007
2. C. Delbos, J. Fazilleau, J.F. Coudert, and P. Fauchais, Plasma Spray Elaboration of Finely Structures YSZ Thin Coating by Liquid Suspension Injection, *Thermal Spray 2003: Advancing the Science & Applying the Technology*, C. Moreau and B. Marple, Eds., (Materials Park, OH), ASM International, 2003, p 661-669
3. T. Poirer, A. Vardelle, M.F. Elchinger, M. Vardelle, A. Grimaud, and H. Vesteghem, Deposition of Nanoparticle Suspensions by Aerosol Flame Spraying: Model of the Spray and Impact Processes, *Thermal Spray 2003: Advancing the Science and Applying the Technology,* Vol 2, B.R. Marple and C. Moreau, Eds., May 5-8, 2003 (Orlando, FL), ASM International, 2003, 393 pages
4. A. Killinger, M. Kuhn, and R. Gadow, High-Velocity Suspension Flame Spraying (HVSFS), A New Approach for Spraying Nanoparticles with Hypersonic Speed, *Surf. Coat. Technol.*, 2006, **201**, p 1922-1929
5. E. Bouyer, F. Gitzhofer, and M. I. Boulos, Powder Processing by Suspension Plasma Spraying, *Thermal Spray: A United Forum for Scientific and Technological Advances,* C.C. Berndt, Ed., Sept 15-18, 1997 (Indianapolis, IN), ASM International, 1998, 353 pages
6. R. Rampon, G. Bertrand, F.-L Toma, and C. Coddet, Liquid Plasma Sprayed Coatings of Yttria Stabilized Zirconia for SOFC Electrolytes, *Proceedings of the 2006 International Thermal Spray Conference* (Seattle, WA), ASM International, 2006
7. H. Kreye, Vergleich der HVOF-Systeme—Werkstoffverhalten und Schichteigenschaften, 4. Kolloquium Hochgeschwindigkeitsflammspritzen, 1997, p 13-21
8. R. Gadow, F. Kern, and A. Killinger, Manufacturing Technologies for Nanocomposite Ceramic Structural Materials and Coatings, *Materials Science and Engineering B,* Vol 148 (No.1-3), P. Kumta, Ed., (Amsterdam), Elseveir B. V., 2008, p 58-64. ISSN 0921-5107